J. Membrane Biol. 125, 49–62 (1992)

The Journal of
Membrane Biology

Electrogenic Properties of the Cloned Na^+/Glucose Cotransporter: I. Voltage-Clamp Studies

Lucie Parent, Stéphane Supplisson, Donald D.F. Loo, and Ernest M. Wright
Department of Physiology, University of California at Los Angeles School of Medicine, Center for the Health Sciences, Los Angeles, California 90024-1751

Summary. The cloned rabbit intestinal Na^+/glucose cotransporter was expressed in *Xenopus laevis* oocytes. Presteady-state and steady-state currents associated with cotransporter activity were measured with the two-electrode voltage-clamp technique. Steady-state sugar-dependent currents were measured between -150 and $+90$ mV as a function of external Na^+ ($[Na]_o$) and α-methyl-D-glucopyranoside concentrations ($[\alpha MDG]_o$). $K_{0.5}^{\alpha MDG}$ was found to be dependent upon $[Na]_o$ and the membrane potential. At $V_m = -50$ mV, increasing $[Na]_o$ from 10 to 100 mM decreased $K_{0.5}^{\alpha MDG}$ from 1.5 mM to 180 μM. Increasing membrane potential toward negative values decreased $K_{0.5}^{\alpha MDG}$ at nonsaturating $[Na]_o$. For instance, at 10 mM $[Na]_o$, $K_{0.5}^{\alpha MDG}$ decreased from 1.5 mM to 360 μM on increasing the membrane potential from -50 to -150 mV. The $i_{max}^{\alpha MDG}$ was relatively insensitive to $[Na]_o$ between 10 and 100 mM and weakly voltage dependent (e-fold increase per 140 mV). $K_{0.5}^{Na}$ and i_{max}^{Na} were found to be dependent upon membrane potential and $[sugar]_o$. In the presence of 1 mM $[\alpha MDG]_o$, $K_{0.5}^{Na}$ decreased from 50 to 5 mM between 0 and -150 mV and i_{max}^{Na} increased twofold between -30 and -200 mV. The voltage dependence of $K_{0.5}^{Na}$ is consistent with an effect of potential on Na^+ binding (Na^+-well effect), whereas the voltage dependence of i_{max}^{Na} is compatible with the translocation step being voltage dependent. It is concluded that voltage influences both Na^+ binding and translocation. Presteady-state currents were observed for depolarization pulses in the presence of 100 mM $[Na]_o$. The transient current relaxed with a half time of $\approx$10 msec, and both the half time and magnitude of the transient varied with the holding potential and the size of depolarization pulse. Presteady-state currents were not observed after the addition of phlorizin or αMDG to the external Na^+ solution and were not observed for water-injected control oocytes. We conclude that presteady-state currents are due to the activity of the carrier and that they may give a novel insight to the transport mechanism of the Na^+/glucose cotransporter.

Key Words Na^+/glucose cotransport · electrogenic cotransporters · steady-state kinetics · presteady-state currents · clone · *Xenopus* oocytes

I. Introduction

Na^+-dependent cotransporters are membrane proteins found mainly in animal cells. Their physiological role is to accumulate organic solutes, e.g., sugars and amino acids, and inorganic solutes within cells. The energy for this process is provided by the electrochemical gradient across the membrane for Na^+ ions, and the process is frequently referred to as secondary active transport (for reviews *see* Semenza et al., 1984; Schultz, 1986; Hopfer, 1987). Whereas it has been long established that Na^+-dependent cotransporters are electrogenic and voltage dependent (for review *see* Schultz, 1986), few studies have directly characterized their electrophysiological properties (Jauch, Petersen & Läuger, 1986; Lapointe, Hudson & Schultz, 1986; Smith-Maxwell et al., 1990).

Throughout the years, models that have been proposed to describe Na^+-substrate cotransport have either featured a voltage-dependent effect on Na^+ binding (Na^+-well model) or an effect of potential on any carrier translocation step (Semenza et al., 1984; Läuger & Jauch, 1986). Studies reporting the effect of potential on steady-state kinetics can provide invaluable information about the mechanism of Na^+/substrate cotransport and the site of the voltage-dependence (Kimmich, 1990). For instance, Jauch and Läuger (1986) have demonstrated, using the whole-cell variant of the patch-clamp technique, that the cotransport of alanine through the Na^+/alanine cotransporter involved a voltage-dependent Na^+/binding reaction step. In the same study, they also showed that the voltage dependence of $K_m^{alanine}$ was only compatible with a simultaneous cotransport model.

The successful cloning and expression of the Na^+/glucose cotransporter activity in *X. laevis* oocytes (Hediger et al., 1987; Ikeda et al., 1989) now makes it possible to investigate the effect of potential on steady-state and presteady-state kinetics using an electrophysiological approach. When expressed in *Xenopus* oocytes, the cloned Na^+/glucose co-

transporter can generate net inward currents up to 500 nA (Umbach, Coady & Wright, 1990) that makes it possible to measure steady-state Na^+/glucose kinetics on a single oocyte. These advantages led us to a comprehensive study of the kinetics of the Na^+/glucose cotransporter as a function of voltage. In addition to steady-state kinetics, we also report our observations on the presteady-state kinetics of the cotransporter. Preliminary reports of these results have been presented elsewhere (Parent et al., 1990*a*,*b*).

II. Materials and Methods

A. cRNA Transcription

Plasmid pMJC424, namely pBluescript KS^+ with a 2.2 kb insert containing the cDNA encoding for the rabbit intestinal Na^+/glucose cotransporter, was cleaved with Not I, and RNA was transcribed and capped as described previously (Hediger et al., 1987).

B. Oocyte Preparation

Stage V or VI oocytes from adult *X. laevis* frogs (Xenopus 1, Ann Arbor, MI) were treated with 5 mg/ml of collagenase-B (Boehringer-Mannheim, Indianapolis, IN) for 1 hr at room temperature (Ikeda et al., 1989). Oocytes were then manually defolliculated after 1-hr incubation in a K-phosphate medium (100 mM K_2HPO_4; 0.1 g/ml bovine serum albumin) and left to recover overnight. They were injected with either 50 (±1) ng of cRNA or diethyl-pyro-carbonate (DEPC) treated H_2O and were cultured at 18°C in a Barth's medium containing (in mM): 88 NaCl, 1 KCl, 0.33 $Ca(NO_3)_2$, 0.41 $CaCl_2$, 0.82 $MgSO_4$, 2.4 $NaHCO_3$, 10 HEPES-Tris, 0.1 mg/ml gentamicin, pH 7.4 for 5 to 14 days. Experiments were performed from July 1989 to August 1990.

C. Electrophysiology

Oocyte currents were measured with the two microelectrode voltage-clamp method. Both electrodes were filled with 3 M KCl with resistances ranging from 7 to 14 MΩ. Although oocyte resting potentials were found to vary from −20 to −70 mV, they were relatively constant for oocytes coming from the same frog. As measured in a Na^+ medium (*see below* for composition), cRNA-injected oocytes usually showed a slightly lower resting potential with a mean membrane potential of −38 mV (SEM = 1; N = 311) as compared to −48 mV (SEM = 2, N = 62) for water-injected oocytes. Only oocytes with a resting potential more negative than −35 mV were used in the experiments described here.

Under voltage-clamp conditions, command potentials were controlled by an IBM-compatible computer (Everex 386/25) via the software CLAMPEX from pCLAMP (version 5.5, Axon Instruments). CLAMPEX was modified to include analysis features such as steady-state *I-V* curve subtraction and printing of current traces. For the experiments described herein, current-voltage (*I-V*) relationships were obtained with a pulse protocol. For most experiments, current-voltage relationships were obtained with 21 pulses of potential (+10-mV increment) between −150 and +50 mV. The oocyte membrane was pulsed at time t = 4 msec to the test potential for 84 msec followed by a 1-sec interpulse interval at the holding potential of −50 mV before the next pulse. Note that test potentials were symmetrically applied around the holding potential. No difference in the *I-V* curve was observed whether the membrane was pulsed from positive-to-negative or from negative-to-positive potentials. Currents were filtered at 20 kHz, digitized at 200 μsec (512 samples) and saved on computer. Steady-state currents were obtained by averaging the current between 72 to 76 msec (20 samples).

The total current measured at steady state may be represented by the sum of the current, i, carried by the Na^+/glucose cotransporter plus the current $i_m = (V_m - V_r)/R_m$ through other conductive pathways in the cell membrane

$$i = i_{\text{measured}} - i_m \tag{1}$$

where R_m is the membrane resistance in the absence of sugar, V_m is the membrane potential and V_r is the resting potential. Implicit in this representation is the assumption that sugar has no other electrical effect apart from activating the cotransport system. Experiments performed with known blockers, e.g., 2 mM ouabain, or 500 μM amiloride, or 5 mM $BaCl_2$, or 5 mM TEACl, or the omission of 1 mM $CaCl_2$, or 2 mM KCl, or 1 mM $MgCl_2$, and the replacement of chloride (75%) by gluconate did not affect the size of sugar-dependent currents.

Membrane currents were measured before and after the addition of sugar to the bath. The steady-state sugar-dependent currents i (reported as the difference in current measured in the presence and in the absence of sugar) were fitted to phenomenological Eqs. (2) and (3) using the software ENZFITTER (version 1.05, Elsevier-Biosoft).

$$i = \frac{i_{\max}^{\text{sugar}}\,[\text{sugar}]_o}{K_{0.5}^{\text{sugar}} + [\text{sugar}]_o} \tag{2}$$

$$i = \frac{i_{\max}^{\text{Na}}\,[\text{Na}]_o^n}{(K_{0.5}^{\text{Na}})^n + [\text{Na}]_o^n} \tag{3}$$

where i is the difference in current measured before and after the addition of sugar (±sugar) at any given test potential, $[\text{sugar}]_o$ is the external sugar and $[\text{Na}]_o$ the external Na^+ ions concentration. n is the apparent coupling coefficient for Na^+ ions, $i_{\max}^{\text{sugar}}$ the maximum current at saturating external sugar concentration, $i_{\max}^{\text{Na}}$ the maximum current at saturating external Na^+ concentration and $K_{0.5}^{\text{sugar}}$ is the external sugar concentration that gives half the value of $i_{\max}^{\text{sugar}}$. $K_{0.5}^{\text{Na}}$ is the external Na^+ concentration that gives half the value of $i_{\max}^{\text{Na}}$. The error on the fit is shown as ± error value such as in Figs. 3 to 10. To distinguish the "error" of the fit (±error) from the statistical error of a group of results, the mean value of a series of experiments will be given in the form: mean (SEM; N) where SEM is the standard error of the mean (SEM = SD/$\sqrt{N}$) and N is the size of the sample.

The kinetic analysis was limited to steady-state sugar-dependent inward currents obtained in the potential range for which $E_{\text{Na}} - E_m \geq 30$ mV at all $[\text{Na}]_o$, given that $[\text{Na}]_i$ is 15 mM (Dascal, 1987). This allows measurement of steady-state sugar-dependent currents in a range where the signal-to-noise ratio is optimum.

Experiments performed throughout the year with 62 water-injected oocytes under voltage-clamp conditions never showed a sugar dependent current greater than 1 nA. In addition, the

maximum uptake of 50 μM [^{14}C]-αMDG in water-injected oocytes as measured in our lab under nonvoltage-clamp conditions was 2 ± 1 pmol oocyte^{-1} hr^{-1}*.

D. Experimental Protocol

Oocytes were always impaled to measure the resting potential and then allowed to stabilize 15 to 20 min before the second electrode impalement. Current-voltage relations (*I-V* curves) were then measured under control conditions in a 100-mM Na^+ medium (*see* section II.E. for composition). Experiments were performed in a 500-μl chamber perfused continuously, except for the 30-sec recording period, at a rate of 8 ml/min. Under these conditions we were able to keep oocytes under voltage clamp for periods as long as 3 hr. The bath solution was then replaced by a test solution (for instance Na^+ medium ± sugar or Na^+-choline medium ± sugar) and a new series of *I-V* relationships was measured. Exposure to the sugar solution was kept as brief as possible (<2 min). As an internal control, membrane potential and whole-cell current were always measured before and after the perfusion of the test solution. Only oocytes for which potential and current returned to the baseline after washout of the sugar solution and return to control conditions were kept for further experiments. The difference between *I-V* curves measured at steady state in the presence and the absence of sugar (±sugar) will be referred to as steady-state sugar-dependent currents.

Unless stated otherwise, experiments were performed at room temperature 18–20°C. For the experiment shown in Figs. 5 and 6, oocyte chamber temperature was controlled by a thermoelectric Peltier unit (Model 940-31, Thermoelectric Cooling America, Chicago, IL) and monitored continuously by a thermocouple (Models 650 and Hyp-0-33, Omega, Stamford, CT).

E. Solutions

For most experiments, oocytes were bathed in Na^+ solution containing (in mM): 100 NaCl, 1 KCl, 1 $CaCl_2$, 1 $MgCl_2$, 10 HEPES-Tris, pH 7.4. For experiments performed with $[Na]_o$ lower than 100 mM, NaCl was replaced isoosmotically by CholineCl. To compare our results with uptake experiments (Ikeda et al., 1989) and to eliminate any interference related to D-glucose metabolism, steady-state sugar-dependent currents were usually measured with α-methyl-glucopyranoside (αMDG) as the substrate (Brot-Laroche et al., 1987). Chemicals (phlorizin, ouabain, amiloride, collagenase) and enzymes were purchased from Sigma (St. Louis, MO), Boehringer-Mannheim (Indianapolis, IN), and Stratagene (La Jolla, CA).

* It is unlikely that the native *Xenopus* oocyte Na^+/glucose transporter reported by Weber, Schwarz and Passow (1989) played a major role in our study. As Weber et al. acknowledged, the addition of 10 mM glucose to a Na-rich medium may trigger a membrane depolarization (1–5 mV) in native oocytes that would amount to less than 1 nA of specific current. We conclude that the native *Xenopus* oocyte Na^+/glucose transporter currents are insignificant as compared to the typical current of 100–200 nA observed in cRNA-injected *Xenopus* oocytes measured in this study.

III. Results

A. Steady-State Sugar-Dependent Currents

Figure 1*A* shows the typical current traces of control water-injected oocytes measured in the 100 mM Na^+ medium in response to voltage pulses from a holding potential of −50 mV. The capacitive current decayed monotonically with a time constant (τ_1) of 1 msec† to a steady-state current level. As seen in the right panel (Fig. 1*B*), addition of 1 mM αMDG to the bathing medium failed to increase the size of steady-state membrane currents.

Figure 1*C* shows current traces recorded in the Na^+ medium with an oocyte obtained from the same frog but injected with cRNA coding for the Na^+/glucose cotransporter. While the water-injected oocyte currents reached a steady-state level with a single time constant of 1 msec, the cRNA-injected oocyte currents relaxed more slowly to a steady-state current at positive potentials. This slower decay (≈10 msec) was systematically observed at positive clamp potentials when bathed in Na^+ medium and will be discussed in more detail later (section III.D.).

Addition of sugar to the bathing medium increased membrane inward currents and eliminated the slow transient component (Fig. 1*D*). The corresponding steady-state current values obtained from traces of Fig. 1*C* and *D* are shown in Fig. 2*A* as a function of the test potential. The difference in membrane currents measured before and after the addition of αMDG is reported in Fig. 2*B*. The addition of sugar shifted the zero current potential from −60 to −15 mV, a shift similar to sugar-induced depolarization observed under nonvoltage-clamp conditions. The addition of sugar caused a threefold increase in the membrane slope conductance as measured between 10 and −70 mV from 0.9 to 2.6 μS. The membrane depolarization and the conductance increase required the presence of Na^+ ions in the

† Given that an oocyte is a sphere of 1-mm diameter with a specific membrane capacitance area of 1 μF cm^{-2}, the oocyte capacitance (C_o) would be 0.031 μF (31 nF). For instance, the charge (Q) associated with a depolarization of ΔV = 60 mV from −50 to +10 mV would be $Q = C_o \cdot \Delta V$ = 1.9×10^{-9} coulomb. From the values of the exponential functions obtained at +10 mV, the charge (Q) associated with the same depolarization step would be equal to $Q = i_1 \cdot \tau_1$ = 0.98 msec · 2 μA = 1.96×10^{-9} coulomb where i_1 is the maximum extrapolated current of the exponential function and τ_1 is its time constant. The physical and calculated values of Q agree reasonably well, considering that the oocyte surface area is underestimated due to the presence of membrane microvilli. It is concluded therefore that τ_1 (1-msec time constant) may correspond to the oocyte-capacitive transient.

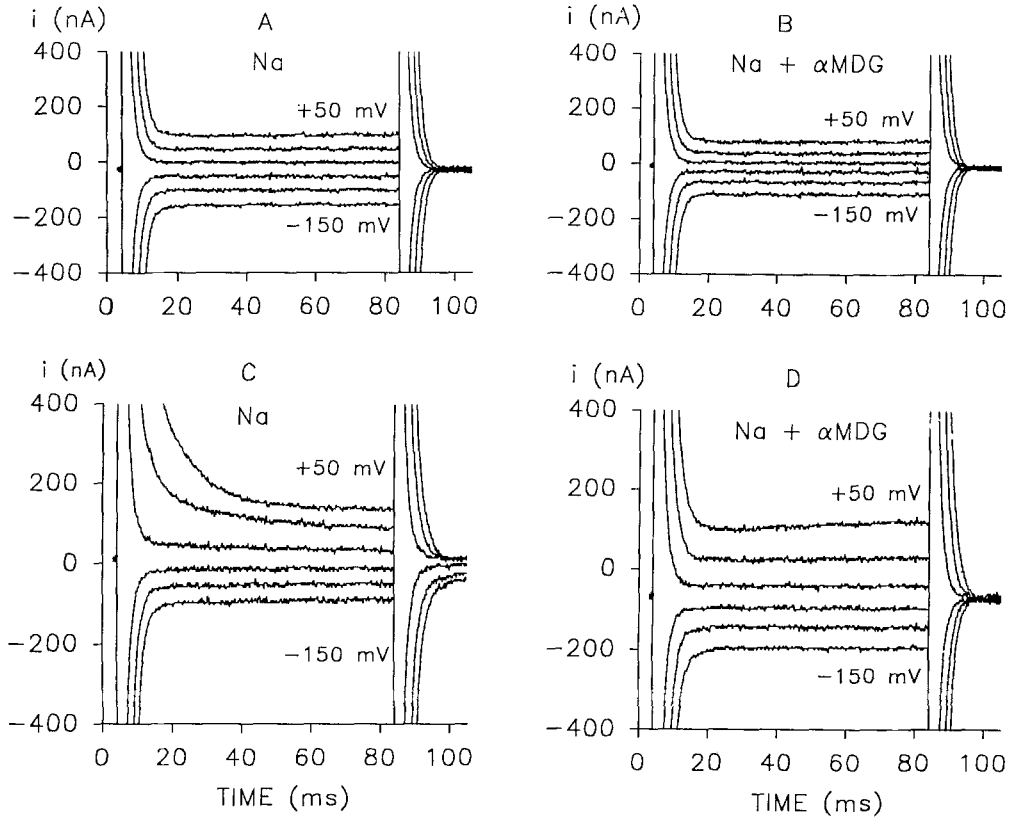

Fig. 1. Current traces recorded in a Na^+ medium are shown before and after the addition of 1 mM αMDG to the bathing medium. The oocyte membrane was held at a holding potential (V_h) of −50 mV. In this experiment and in all subsequent records, the test potential was applied at 4 msec for 84 msec. The six test potentials shown are −150, −110, −70, −30, 10, and 50 mV. RNA-injected and water-injected oocytes were from the same frog, and both experiments were performed the seventh day after injection. The bathing solution was the Na^+ medium containing (in mM): 100 NaCl, 2 KCl, 1 $MgCl_2$, 1 $CaCl_2$, 10 HEPES-Tris, pH 7.4. (*A*) and (*B*) Water-injected oocyte. Steady-state current values were not affected by the sugar addition. (*C*) and (*D*) RNA-injected oocytes. Addition of 1 mM αMDG triggered an increase in steady-state inward current for the cRNA-injected oocyte (*D*). The developing outward current at +50 mV is due to a native voltage and time-activated conductance and was only observed from time to time. Steady-state current values are shown as a function of potential in Fig. 2. Note that the current traces in RNA-injected oocytes bathed in the presence of 100 mM Na^+ medium decay more slowly to the steady state at positive potentials compared with those obtained in the presence of sugar (*D*) and those in water-injected oocytes (*A*) and (*B*). *See* Fig. 8 for further analysis of these current transients.

bathing medium and was blocked by addition of 100 μM phlorizin (*results not shown*). As seen, the steady-state sugar-dependent *I-V* curve was sigmoidal with no measurable reversal potential. This *I-V* curve shape is typical of this series of experiments (*see* Figs. 3 and 5).

B. Voltage Dependence of i_{max} and $K_{0.5}$ for Sugar

To evaluate the voltage-dependence of Na^+/glucose kinetics, steady-state sugar-dependent currents were measured as a function of extracellular sugar and Na^+ ion concentrations. Steady-state currents were measured as a function of external sugar while keeping extracellular Na^+ constant. In some instances, experiments were successfully conducted where steady-state sugar-dependent currents were measured both as a function of $[\alpha MDG]_o$ and $[Na]_o$ on a single oocyte.[1] The results of such an experiment are shown in Fig. 3. Steady-state sugar-dependent currents were measured at fixed $[Na]_o$ from 10 to 100 mM while $[\alpha MDG]_o$ was varied from 20 μM to 20 mM. One typical set of current-voltage relation-

[1] There are variations in the number of carriers expressed per oocyte in the two- to fivefold range. Such variations influence proportionally the absolute magnitude of i_{max} and of the peak presteady-state currents (*see below*). $K_{0.5}$ however are independent of the number of carriers expressed as the experimental data reported in the companion paper (Fig. 6) show.

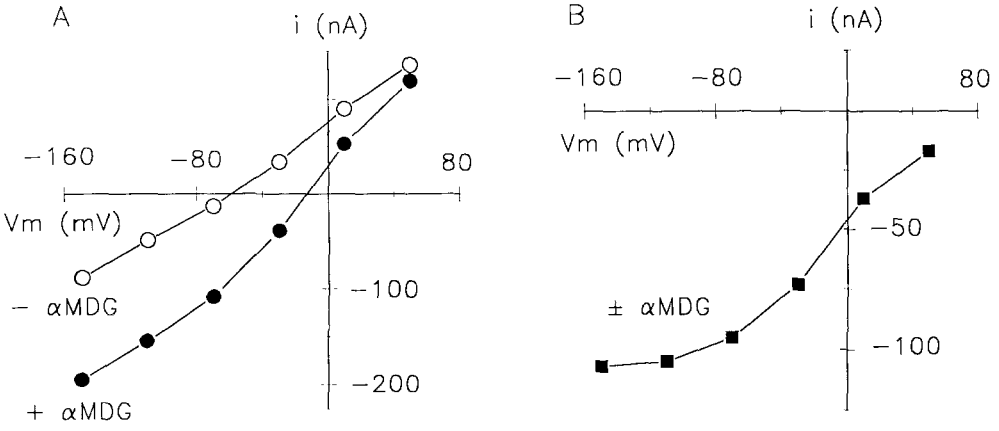

Fig. 2. Steady-state current-voltage relations of the sugar-coupled inward Na^+ currents in cRNA-injected oocytes. The current values were averaged from 20 points between 72 and 76 msec from the experimental data shown in Fig. 1*C* and *D*. (*A*) Current-voltage relationships obtained with (in mM): 100 NaCl, 2 KCl, 1 $MgCl_2$, 1 $CaCl_2$, 10 HEPES-Tris, pH 7.4 in the absence (○) and in the presence of 1 mM $[\alpha MDG]_o$ (●). (*B*) Steady-state sugar-dependent current-voltage relationships were obtained by taking the difference between the current obtained before (○) and after (●) the addition of 1 mM αMDG to the bathing solution. Unless indicated otherwise, the lines between symbols were drawn by eye in this figure and the following ones.

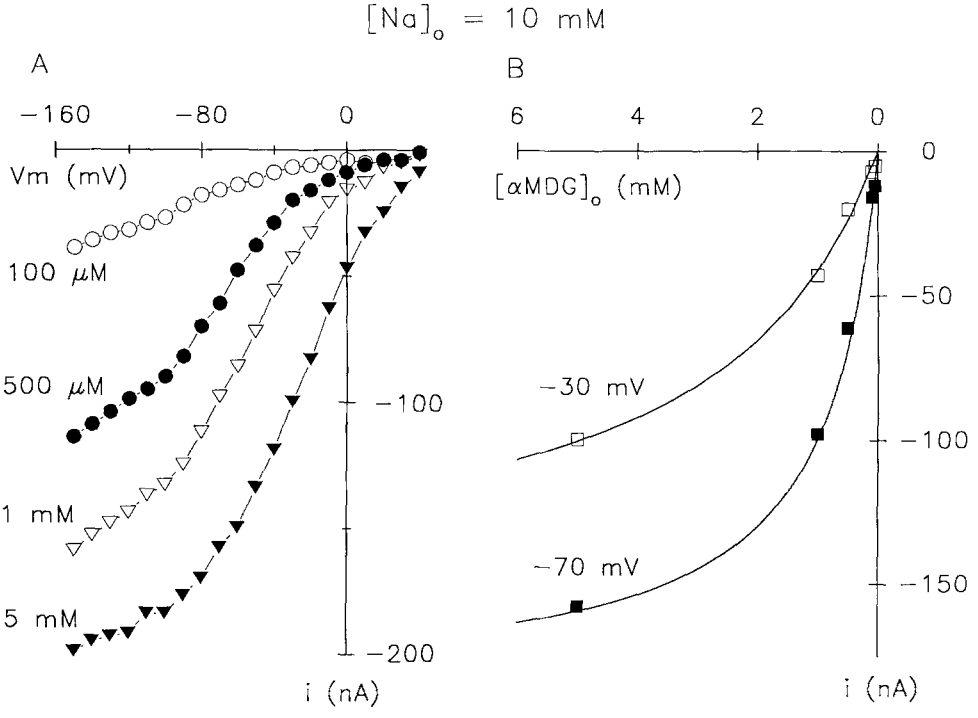

Fig. 3. Steady-state sugar-dependent currents as a function of $[\alpha MDG]_o$ in a single cRNA-injected oocyte. (*A*) Current-voltage relationships were obtained for each sugar concentration as shown in Figs. 1 and 2 with (in mM): 10 NaCl, 90 cholineCl, 2 KCl, 1 $MgCl_2$, 1 $CaCl_2$, 10 HEPES-Tris, pH 7.4, and varying $[\alpha MDG]_o$ from 50 μM to 10 mM. Four out of the eight αMDG concentrations actually tested are shown. The *I-V* curves were sigmoidal, approaching saturation at high negative potentials especially at 5 mM $[\alpha MDG]_o$ and asymptoting towards zero at positive potentials. (*B*) Steady-state sugar-dependent currents were plotted as a function of $[\alpha MDG]_o$ at −70 mV (□) and −30 mV (■). The curves were fitted to Eq. (2) with the following parameter values: at −70 mV, $i_{max}^{\alpha MDG} = 188 \pm 11$ nA and $K_{0.5}^{\alpha MDG} = 0.89 \pm 0.14$ mM and at −30 mV, $i_{max}^{\alpha MDG} = 157 \pm 12$ nA and $K_{0.5}^{\alpha MDG} = 2.8 \pm 0.3$ mM. These kinetic parameters are included in the larger data set shown in Fig. 4.

ships is shown in Fig. 3*A* in which steady-state sugar-dependent *I-V* curves were measured with $[Na]_o$ fixed at 10 mM as a function of eight different $[\alpha MDG]_o$ starting from the lowest (50 μM) to the highest (10 mM). Four current-voltage curves out of the eight are shown here. Note the absence of outward currents for all *I-V* curves. For all potentials investigated, steady-state sugar-dependent currents increased hyperbolically as a function of $[\alpha MDG]_o$. A maximum current of −200 nA was measured with 5 mM $[\alpha MDG]_o$ at V_m = −150 mV. This current is identical to the one obtained in the same experiment with 1 mM $[\alpha MDG]_o$ and 100 mM $[Na]_o$ at the same potential (*results not shown*). At high αMDG concentrations (>500 μM) the *I-V* curves were linear between −90 to −50 mV and showed saturation behavior at more negative potentials. Steady-state sugar-dependent currents obtained as a function of $[\alpha MDG]_o$ were well described by Eq. (2).[2] Results are shown in Fig. 3*B* for −30 and −70 mV. Increasing the membrane potential from −30 to −70 mV caused $K_{0.5}^{\alpha MDG}$ to decrease from 2.8 ± 0.3 to 0.89 ±0.14 mM and $i_{max}^{\alpha MDG}$ to increase from −157 ± 12 to −188 ± 11 nA. From the complete set of results shown in Fig. 4*A*, it can be seen that at 10 mM $[Na]_o$, $K_{0.5}^{\alpha MDG}$ was voltage dependent over the −20 to −150 mV range with a negative membrane potential decreasing $K_{0.5}^{\alpha MDG}$. The apparent $i_{max}^{\alpha MDG}$ showed a lower voltage dependence, being linear between −50 and −90 mV (*e*-fold change per 160 mV) and saturating at more negative potentials.

The entire set of results obtained for this experiment is shown in Fig. 4. $K_{0.5}^{\alpha MDG}$ was dependent upon $[Na]_o$ at any given potential. For instance, $K_{0.5}^{\alpha MDG}$ decreased from 7.2 mM in the presence of 2 mM $[Na]_o$ to 200 μM when measured with 100 mM $[Na]_o$ (V_m = −70 mV). The Na dependence of $K_{0.5}^{\alpha MDG}$ decreased, however, as the potential was made more negative. At V_m = −150 mV, $K_{0.5}^{\alpha MDG}$ decreased from 360 ± 13 μM to 230 ± 11 μM between 10 and 100 mM $[Na]_o$. As the $[Na]_o$ decreased, the voltage dependence of $K_{0.5}^{\alpha MDG}$ became steeper. At 10 mM $[Na]_o$, $K_{0.5}^{\alpha MDG}$ increased 2.5-fold from 360 ± 13 to 885 ± 15 μM between −150 and −70 mV, whereas at 2 mM $[Na]_o$ $K_{0.5}^{\alpha MDG}$ increased fivefold from 1.3 to 7.2 mM over the same potential range.

To summarize, $K_{0.5}^{\alpha MDG}$ was found to decrease as $[Na]_o$ increased and as the membrane potential was made more negative. The effect of membrane potential was stronger at low $[Na]_o$ (2 to 30 mM).

The corresponding values of $i_{max}^{\alpha MDG}$ obtained during the same experiment were plotted as a function of potential in Fig. 4*B*. $i_{max}^{\alpha MDG}$ was weakly dependent upon membrane potential and varied little with $[Na]_o$. For $[Na]_o$ between 10 and 100 mM, $i_{max}^{\alpha MDG}$ decreased with an *e*-fold change per 160 mV between −10 and −90 mV and the voltage sensitivity was

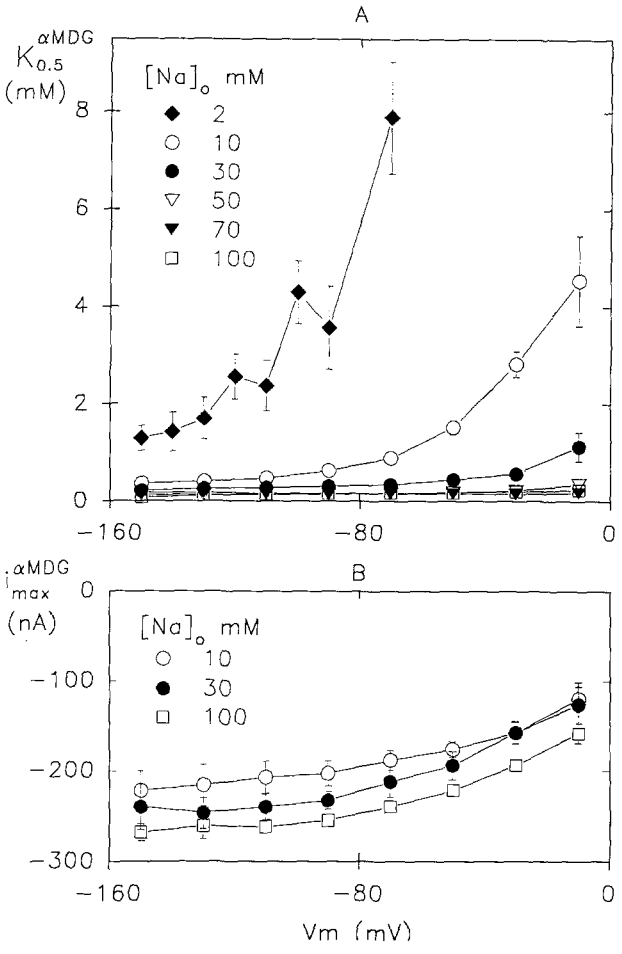

Fig. 4. Voltage dependence of $i_{max}^{\alpha MDG}$ and $K_{0.5}^{\alpha MDG}$ as a function of $[Na]_o$. In one cRNA-injected oocyte, $[Na]_o$ was varied from 10 to 100 mM (cholineCl substitution), and at each $[Na]_o$, $[\alpha MDG]_o$ was varied between 20 μM to 10 mM. (*A*) Voltage dependence of $K_{max}^{\alpha MDG}$ was a function of $[Na]_o$. At 100 mM $[Na]_o$, $K_{0.5}^{\alpha MDG}$ was 73 ± 20 μM (−150 mV), 177 ± 6 μM (−50 mV), and 233 ± 45 μM (−10 mV). At 10 mM $[Na]_o$ $K_{0.5}^{\alpha MDG}$ was 0.36 ± 0.13 mM (−150 mV), 1.5 ± 0.15 mM (−50 mV), and 4.6 ± 0.9 mM (−10 mV). $[Na]_o$ were (in mM): 10 (○), 30 (●), 50 (△), 70 (▲), and 100 (□). Also included are the results of a separate experiment performed with 2 mM (◆) $[Na]_o$. (*B*) Voltage dependence of $i_{max}^{\alpha MDG}$ as a function of $[Na]_o$. At 100 mM $[Na]_o$ $i_{max}^{\alpha MDG}$ was −268 ± 9 nA (−150 mV), −222 ± 4 nA (−50 mV), and −158 ± 11 nA (−10 mV). At 10 mM $[Na]_o$ $i_{max}^{\alpha MDG}$ was −222 ± 22 nA (−150 mV), −176 ± 9 nA (−50 mV), and −120 ± 14 nA (−10 mV). $i_{max}^{\alpha MDG}$ increased slightly with potential between −90 and −150 mV but the steepest increase was observed between −10 and −90 mV. $i_{max}^{\alpha MDG}$ values obtained for $[Na]_o$ between 10 and 100 mM were not found to be significantly different at each potential (t < 95%). Symbols are (in mM) 10 (○), 30 (●) and 100 (□) $[Na]_o$. Error bars represent the error on the fit.

[2] When the fit was performed with a nonlinear Hill-type equation such as Eq. (3), the Hill coefficient n was found to be 1.2 ± 0.2 at −70 mV ($K_{0.5}^{\alpha MDG}$ = 0.74 ± 0.15 mM and $i_{max}^{\alpha MDG}$ = 175 ± 15 nA) and n = 1.0 ± 0.3 at −30 mV ($K_{0.5}^{\alpha MDG}$ = 2.7 ± 1.4 mM and $i_{max}^{\alpha MDG}$ = 153 ± 51 nA).

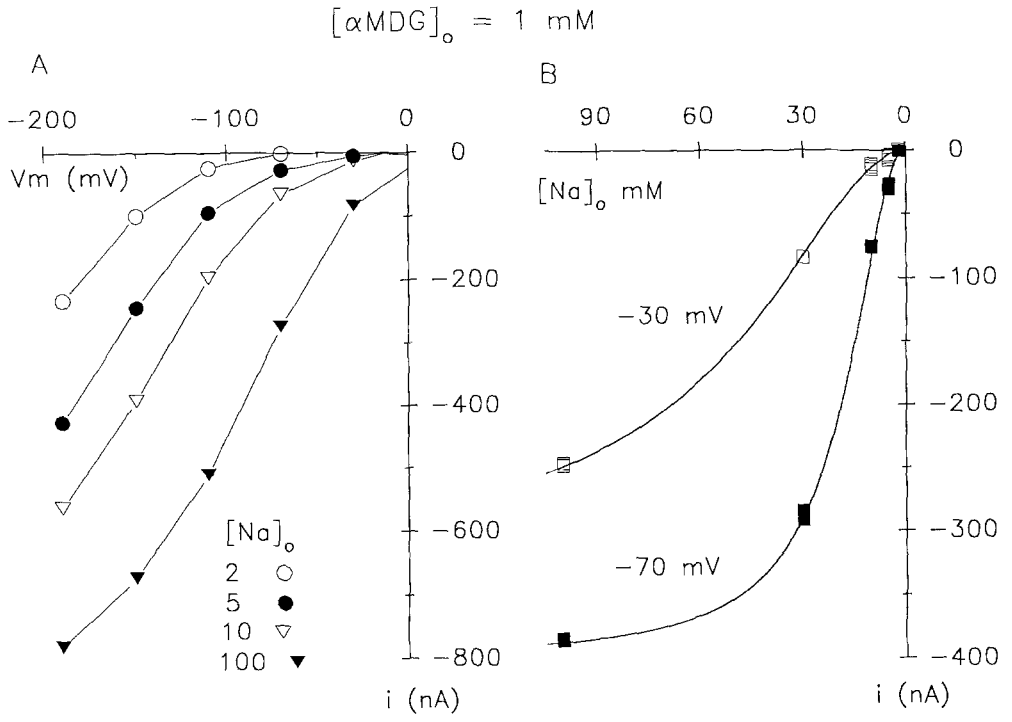

Fig. 5. Steady-state sugar-dependent currents measured as a function of $[Na]_o$. (*A*) Current-voltage relationships were obtained with $[\alpha MDG]_o$ fixed at 1 mM, and $[Na]_o$ varied from 2 to 100 mM in a single cRNA-injected oocyte. CholineCl was substituted for NaCl. The experiment was performed at 32°C with six external [Na]. Only four $[Na]_o$ are shown. Note the sigmoidal shape of the curves. (*B*) Steady-state sugar-dependent currents were plotted as a function of $[Na]_o$ at −70 mV (■) and −30 mV (□). The curves were drawn according to Eq. (3) with the following parameter values: at −70 mV, $n = 2.1 \pm 0.1$, $i_{max}^{Na} = 400 \pm 9$ nA and $K_{0.5}^{Na} = 19 \pm 1$ mM and at −30 mV, $n = 1.9 \pm 0.1$, $i_{max}^{Na} = 324 \pm 17$ nA and $K_{0.5}^{Na} = 53 \pm 2$ mM. The complete set of results is shown in Fig. 6.

less important at membrane potentials more negative than −90 mV. $i_{max}^{\alpha MDG}$ was also found to be slightly sensitive to $[Na]_o$. At −50 mV, $i_{max}^{\alpha MDG}$ was −176 ± 42 nA at 10 mM $[Na]_o$ and was −222 ± 4 nA at 100 mM $[Na]_o$.

C. Voltage Dependence of i_{max} and $K_{0.5}$ for External [Na]

The following series of experiments was performed to determine the voltage dependence of $K_{0.5}^{Na}$ and i_{max}^{Na}. Sugar-dependent inward currents were measured at fixed $[\alpha MDG]_o$ as $[Na]_o$ was varied from 2 to 100 mM.

Steady-state sugar-dependent currents were measured at 0.1, 1 and 20 mM $[\alpha MDG]_o$. Results of an experiment performed with 1 mM $[\alpha MDG]_o$ at 32°C are shown in Fig. 5*A*. Current-voltage relationships appeared sigmoidal especially at 100 mM $[Na]_o$. There was no measurable outward current. Inward currents obtained at a given potential were fitted to Eq. (3) as a function of $[Na]_o$. Curves obtained for potentials −30 and −70 mV are shown in Fig. 5*B*. The relationship between steady-state sugar-dependent currents and $[Na]_o$ was best described by a sigmoidal function. Accordingly, for $V_m = -30$ and −70 mV, the best fit was obtained with n of 1.9 ± 0.1 and 2.1 ± 0.1, $K_{0.5}^{Na}$ decreased from 53 ± 3 to 19 ± 1 mM and i_{max}^{Na} increased from −323 ± 3 to −400 ± 9 nA. Figure 6 shows the complete set of kinetic parameters obtained for that experiment. The best fit was obtained with an apparent coupling coefficient n of 1.9 (SEM = 0.2; $N = 5$) over the complete potential range (Fig. 6*A*). $K_{0.5}^{Na}$ was voltage dependent, decreasing from 53 ± 3 to 3 ± 0.5 mM from −30 to −200 mV (Fig. 6*B*). From this experiment at 32°C and four others at 22°C, $K_{0.5}^{Na}$ was found to decrease from 45 (SEM = 6; $N = 5$) to 17 mM (SEM = 1; $N = 5$) between −30 and −70 mV. i_{max}^{Na} was weakly voltage dependent, increasing by e-fold per 170 mV (Fig. 6*C*).

$K_{0.5}^{Na}$ was also dependent on the external sugar concentration. In separate experiments, increasing $[\alpha MDG]_o$ from 0.1 to 20 mM caused $K_{0.5}^{Na}$ to decrease from 30 ± 7 to 5 ± 1 mM at $V_m = -70$ mV and from 14 ± 5 to 1 ± 1 mM at $V_m = -150$ mV.

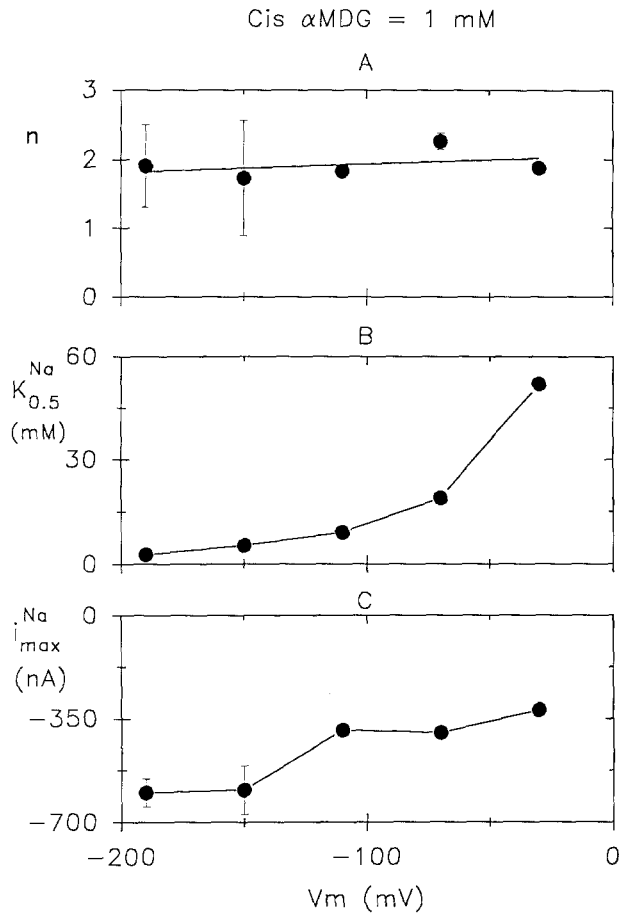

Fig. 6. Voltage dependence of n, i^{Na}_{max} and $K^{Na}_{0.5}$ from the experiment described in Fig. 5. (*A*) The apparent coupling coefficient n was voltage independent with values ranging from a minimum of 1.7 ± 0.8 (−150 mV) to a maximum of 2.3 ± 0.1 (−70 mV). (*B*) $K^{Na}_{0.5}$ decreased with negative potentials from 53 ± 2 mM (−30 mV) to 2.7 ± 0.5 mM (−190 mV). Errors on the fit were smaller than the symbols. (*C*) i^{Na}_{max} increased with negative potentials with an e-fold change per 160 mV from −321 ± 9 nA (−30 mV) to −600 ± 47 nA (−190 mV).

D. Presteady-State Currents

One of the most exciting observations of this study was the recording of presteady-state currents associated with the cotransporter. As observed in Fig. 1, current traces obtained from voltage-clamped RNA-injected oocytes typically show a slower relaxation (Fig. 1*C*) than water-injected oocytes (Fig. 1*A*) in response to a positive voltage pulse to +50 mV.

Only current traces recorded for positive voltages in the presence of 100 mM Na^+ (Fig. 7*A*) exhibited these slow transients. There were no observable transients in the other test groups: nominal absence of Na^+ (Fig. 7*D*), in the presence of Na^+ and sugar (Fig. 7*C*), and in the presence of 100 μM phlorizin[3] (Fig. 7*B*). The threshold Na^+ concentration for observation of current transient was 50 mM. Current transients measured in the presence of high Na^+ were unaffected by the addition of 2 mM ouabain, 400 μM amiloride, 5 mM $BaCl_2$, 5 mM TEACl, and 5 mM DIDS (*results not shown*). From all these observations, it was inferred that current transients were linked to the Na^+/glucose cotransporter activity under presteady-state conditions.

Current traces obtained at V_m = +50 mV in Na^+ medium were fitted to a sum of two exponential functions[4] of τ_{fast} or τ_1 = 1.3 msec and τ_{slow} or τ_2 = 13 msec with corresponding maximum currents i_{fast} or i_1 = 5000 and i_{slow} or i_2 = 900 nA (Fig. 8*A*). The half time constant τ_1 (1.3 msec) was also observed in water-injected oocytes and was identified as the oocyte-capacitive transient (*see* footnote 2). Presteady-state currents of the Na^+/glucose cotransporter were identified by a slower time constant τ_2 of 13 msec. In addition, the fast time constant τ_1 = 1.2 msec (i_o = 6000 nA) was the only time constant measured in presence of phlorizin (Fig. 8*B*).

Presteady-state currents can be observed at potentials more positive than the holding potential, V_h = −50 mV. The parameters of the fast and the slow exponential functions are reported in Fig. 9*A* and *B*. The time constant, τ_1 (capacitive transient), was not found to be significantly voltage dependent with values ranging from 2.3 to 0.95 msec between 50 and −150 mV, whereas τ_2 (carrier presteady-state current) was voltage dependent, decreasing 4.5-fold from 18 to 4 msec between 50 and −30 mV. It was almost impossible to distinguish two time constants at potentials more negative than the holding potential. The maximum current i_1 and i_2 are shown in the right panel (Fig. 9*B*). Currents i_1 and i_2 increased with the amplitude of the voltage step from a fixed holding potential V_h = −50 mV.

Finally, the size of presteady-state currents was also found to be conditioned by the holding potential as shown in Fig. 10. In one experiment, presteady-state currents were measured at a fixed test potential of +50 mV from a holding potential V_h varying between −100 and 0 mV. In this instance, presteady-state currents were reported as the difference between the current measured at τ_2 (10 msec) and the

[3] Addition of 100 μM phlorizin to a 100-mM Na^+ medium also decreased the magnitude of currents measured at steady state. These phlorizin-sensitive Na-dependent currents indicate some Na^+ translocation in the absence of sugar. They represent 5 to 15% of the sugar- and Na-dependent currents.

[4] The determination of presteady-state time constants relies critically on the speed of the voltage-clamp amplifier. In many experiments, it was impossible to voltage clamp adequately the first 5 msec after the pulse onset. Although lack of resolution at these short times does not impair the steady-state data, perfect time resolution was required for presteady-state current evaluation. Therefore, only experiments where the voltage was clamped at 1 msec after the pulse onset were considered.

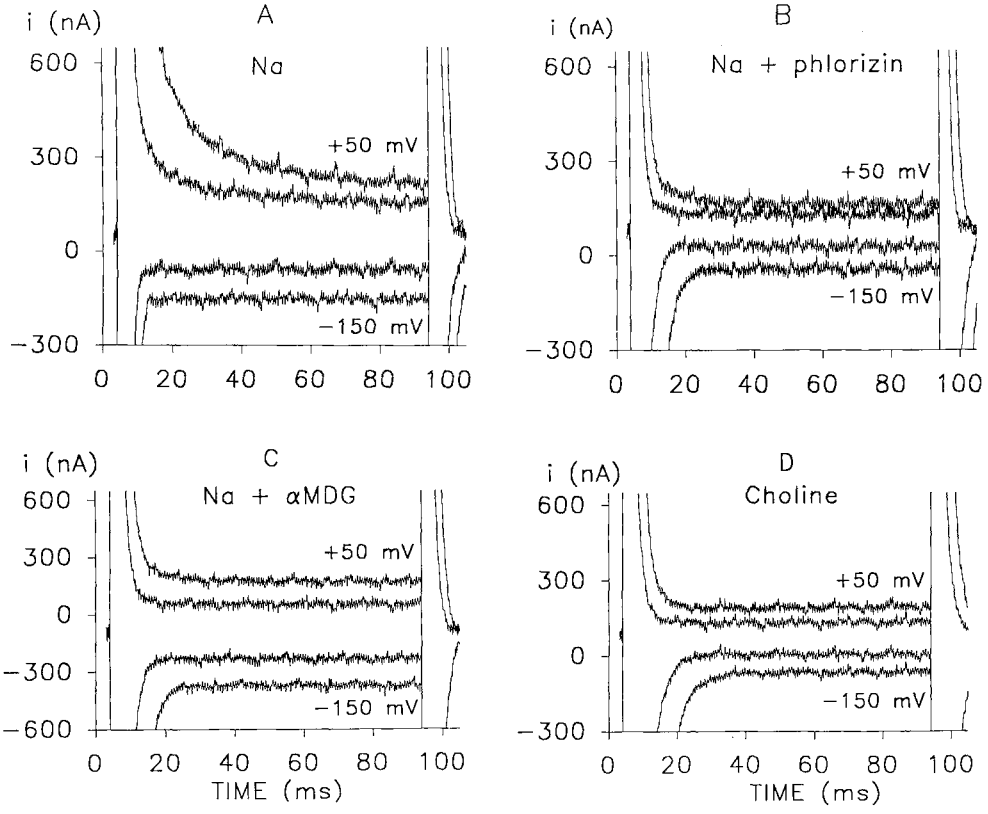

Fig. 7. Na^+/glucose cotransporter presteady-state currents. Current traces were recorded at four 84-msec test potentials (−150, −110, 10, and 50 mV) from a holding potential, V_h, of −50 mV. Records were obtained in the same experiment: (*A*) in 100 mM $[Na]_o$, (*B*) in 100 mM $[Na]_o$ and 100 μM phlorizin, (*C*) in 100 mM $[Na]_o$ and 1 mM $[\alpha MDG]_o$, and (*D*) in 100 mM cholineCl medium (nominal absence of external Na^+). Only current traces recorded in 100 mM Na^+ medium show slow transients. Note the change of scale for the 100 mM $[Na]_o$ and 1 mM $[\alpha MDG]_o$ current traces (*C*). At $V_m = -150$ mV, steady-state currents were (*A*) −155 nA, (*B*) −136 nA, (*C*) −373 nA, and (*D*) −126 nA. Steady-state phlorizin-sensitive currents ($Na^+ \pm$ phlorizin) were −19 nA which is 9% of the steady-state sugar-dependent currents of −218 nA measured at the same potential.

steady-state current (76 msec). Presteady-state currents appear as rectifying outward currents. The more negative the holding potential, the larger the presteady-state current, e.g., as measured at a membrane potential of +90 mV, the transient outward current increased from 28 nA for a holding potential of 0 mV to 97 nA for a holding potential of −100 mV.

IV. Discussion

The purpose of this investigation was to obtain a complete description of the kinetics of the intestinal Na^+/glucose cotransporter as a function of the *cis* Na^+ and sugar concentrations and of the membrane potential. Experiments were specifically designed to yield the maximum kinetic information ($K_{0.5}^{\alpha MDG}$, $i_{max}^{\alpha MDG}$, $K_{0.5}^{Na}$, i_{max}^{Na}) in single oocytes over a wide range of membrane potentials (−30 to −200 mV). In addition, unique kinetic information was obtained from the analysis of presteady-state current transients in the millisecond time scale. Altogether, steady-state and presteady-state findings constitute a comprehensive set of data which were used to develop the Na^+/glucose transport model described in the companion paper. As will be seen, the presteady-state and steady-state electrical properties of the Na^+/glucose cotransporter can be explained by a transport model with an effect of voltage on both ion binding and carrier translocation (Parent et al., 1991*a*,*b*). Experimental results that constitute the basis for the transport model are reviewed below.

A. Sugar-Dependent Steady-State Currents

The cloned intestinal Na^+/glucose cotransporter was expressed in *Xenopus* oocytes, and transport was assayed by measuring inward currents under voltage-clamped conditions. In cRNA-injected oocytes, the addition of αMDG to a Na^+ solution depo-

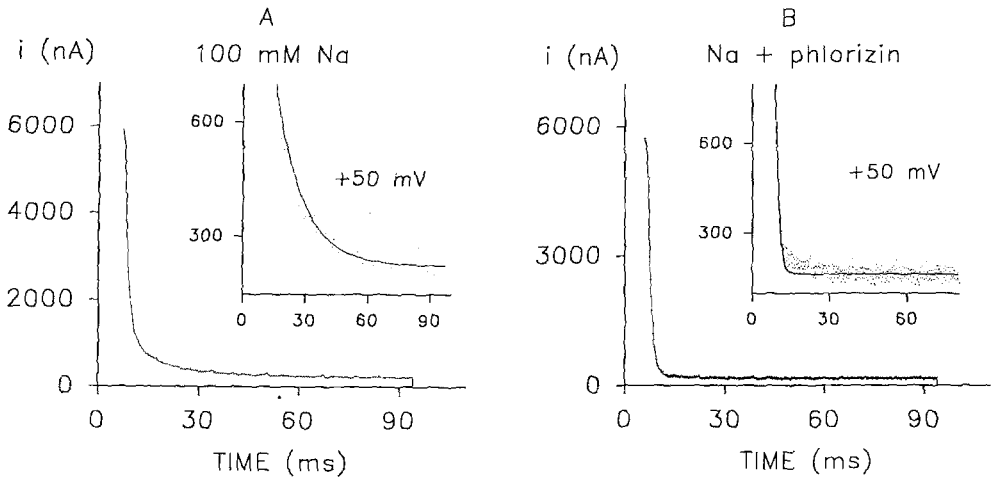

Fig. 8. Presteady-state current time constants. Current traces obtained from the experiment shown in Fig. 7, in the presence of the Na^+ medium before (*A*) and after the addition of 100 μM phlorizin (*B*) to the bath. (*A*) Current traces (dots) obtained at +50 mV were fitted to a sum of two exponential functions (solid line). The same data are shown with an expanded scale in the insert. In the absence of phlorizin, the fitting parameters were τ_1 = 1.3 msec, τ_2 = 13 msec, i_1 = 5000 nA, i_2 = 900 nA. The 1.3-msec time constant was identified as the capacitive time constant. Currents i_1 and i_2 were the current values extrapolated at time zero as given by the fitting procedure for exponential 1 and 2, respectively. (*B*) After the addition of 100 μM phlorizin, the second exponential function (τ_2) was not observed. The exponential function parameters were τ_1 = 1.2 msec and i_1 = 6000 nA. The effect of phlorizin on τ_2 was totally reversible. Note that the time zero of the time axis does not coincide with the time zero of the exponential function. The potential is stepped at 4.2 msec, and the experimental point at 7.2 msec was the first point fitted by the exponential function. The current maximum (i_1) given by the fitting procedure underestimates the actual current extrapolated at the beginning of the pulse.

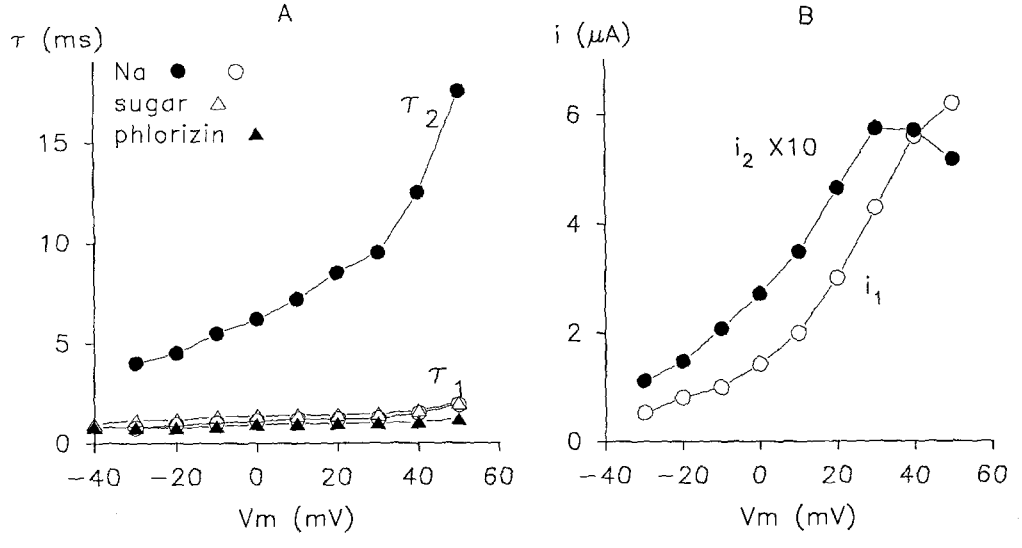

Fig. 9. Dependence of presteady-state current time constants on membrane potential. (*A*) Voltage dependence of time constants was measured under three different experimental conditions: Na^+ medium, Na^+ medium + 100 μM phlorizin, and Na^+ medium + 1 mM αMDG. The holding potential, V_h, was −50 mV. Two exponential functions τ_2 (●) and τ_1 (○) were observed in Na^+ medium. Presteady-state current time constants (τ_2) were only found for depolarization steps and increased with the size of the potential step. In contrast, only one exponential function (τ_1) was observed after the addition of phlorizin (▲) or the addition of αMDG (△) to the Na^+ medium with τ_1 values of 1.9 and 2 msec, respectively, at +50 mV. (*B*) Voltage dependence of currents i_1 and i_2. The magnitude of i_2 and i_1 were directly proportional to the potential step. Note that the current scale is in μA. Current i_2 actually ranged from 0 to 0.6 μA and is shown 10 times bigger than its actual size. Current i_1 ranged from 0 to 6 μA.

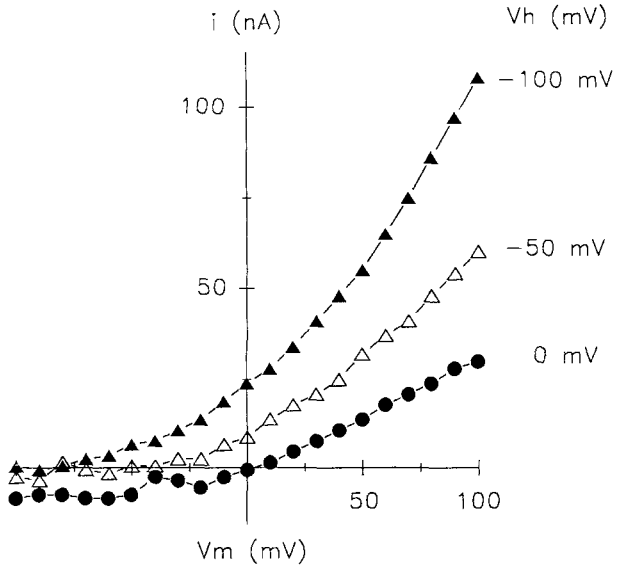

Fig. 10. Dependence of presteady-state current on holding potential. Holding potentials, V_h, were varied from −100 to 0 mV, and currents were recorded in Na^+ medium at test potentials between −150 to +100 mV. Presteady-state currents were reported as the difference between the current measured at 10 msec (roughly at τ_2) (to minimize the interference by the capacitive transient) and the current measured at steady-state (76 msec). Presteady-state currents arise as rectifying-outward currents. The more negative the holding potential, the greater the presteady-state current. As measured at a clamp potential of +90 mV, the transient outward current increased from 28 nA for a holding potential of 0 mV to 97 nA for a holding potential of −100 mV.

larized the membrane potential and increased the membrane conductance (Fig. 2; Umbach et al., 1990; Birnir, Loo & Wright, 1991).Under voltage-clamp conditions, sugar increased inward currents, and this increase was reversibly blocked by 100 μM phlorizin, a specific inhibitor of the Na^+/glucose cotransporter (K_i = 10 μM; Ikeda et al., 1989; Birnir et al., 1991). In the absence of sugar, phlorizin also inhibited a distinct component of the cotransporter, current flowing through the cotransporter, but this sodium-dependent current amounted to less than 15% of the sugar-dependent current (Fig. 7; Umbach et al., 1990). This indicates that the cotransporter is able to carry current, albeit inefficiently, in the absence of sugar.

1. I-V Curves

The sugar-dependent *I-V* curves were sigmoidal (*see also* Umbach et al., 1990; Birnir et al., 1991). The currents approached asymptotically to zero at positive membrane potentials, and in this series of experiments, outward currents were not generally observed (Figs. 2, 3 and 5). At high negative potentials (−150 mV), the inward currents approached saturation (Figs. 2, 3 and 5). The absence of outward currents suggests that there was no sugar accumulation in these oocytes during the experiments[5], and the saturation of the *I-V* curves at high negative potentials indicates the presence of both voltage-sensitive and voltage-insensitive steps in the transport cycle.

In a substantial number of experiments, it was possible to measure sugar-dependent *I-V* curves in a single oocyte over a wide range of external sugar and/or Na^+ concentration without significant changes in the background currents.

2. Sugar-Dependent Currents as a Function of the External Sugar Concentration at Fixed External Na^+ Concentrations

At each fixed external Na^+ concentration and membrane potential the currents were a saturable function of the external sugar concentration (Fig. 3). The data were fitted by a Michaelis-Menten type equation, Eq. (2), which suggests that there is only one sugar binding site on the cotransporter. At 100 mM $[Na]_o$ and −50 mV, an apparent affinity constant for αMDG, $K_{0.5}^{\alpha MDG}$ of 230 ± 50 μM (N = 6), was measured which is comparable to that obtained previously for αMDG uptake and αMDG currents in *Xenopus* oocytes (Ikeda et al., 1989; Birnir et al., 1991).

3. $K_{0.5}^{\alpha MDG}$ and $i_{max}^{\alpha MDG}$ as a function of $[Na]_o$

At −50 mV, $K_{0.5}^{\alpha MDG}$ increased as $[Na]_o$ decreased without a significant change in $i_{max}^{\alpha MDG}$ (Fig. 4), e.g., $K_{0.5}^{\alpha MDG}$ increased from 0.23 to 1.52 mM when $[Na]_o$ was reduced from 100 to 10 mM. Similar $K_{0.5}^{\alpha MDG}$ results were obtained by Birnir et al. (1991) using this system and by Kaunitz and Wright (1984) when they measured glucose uptake into BBMV (brush-border membrane vesicles). This suggests that external Na^+ alters the apparent affinity of the Na^+/glucose cotransporter for external sugar. This allosteric effect of $[Na]_o$ suggests an ordered binding mechanism rather than a random one. Evidence in support of a Na^+-induced conformational change at the sugar binding site was obtained from biophysical studies of extrinsic fluorescence probes covalently attached to lysine residues near the active site (Peerce & Wright, 1984).

[5] In previous experiments where oocytes were preloaded with αMDG, phlorizin-sensitive outward currents were recorded in a sugar-free bathing medium (Umbach et al., 1990).

4. $K_{0.5}^{Na}$, i_{max}^{Na}, and n

At fixed external αMDG concentrations, sugar-activated currents were measured as a function of $[Na]_o$. With 1 mM $[\alpha MDG]_o$ at both 32 and 22°C, the currents were a sigmoidal function of $[Na]_o$ with a Hill coefficient n close to 2. For example, it can be deduced from Fig. 6, that at −50 mV, $n = 2$, $K_{0.5}^{Na} = 30$ mM and $i_{max}^{Na} = -350$ nA. In previous studies of αMDG uptakes with oocytes under nonvoltage-clamp conditions, the Hill coefficient and $K_{0.5}^{Na}$ were 1.5 and 32 mM (Ikeda et al., 1989).

The Na^+-to-sugar coupling coefficient n has been controversial but it should be noted that in chicken enterocytes under voltage-clamped conditions (K gradient in presence of valinomycin), simultaneous αMDG and Na^+ fluxes yield n of 2 (Kimmich & Randles, 1984). A coupling coefficient n of 2 was also inferred from both fluxes (Misfeldt & Sanders, 1982) and reversal potential measurements (Smith-Maxwell et al., 1990) in a cultured renal cell line (LLC-PK_1).

$K_{0.5}^{Na}$ and i_{max}^{Na} were also dependent upon $[\alpha MDG]_o$. Increasing $[\alpha MDG]_o$ from 0.1 to 20 mM caused $K_{0.5}^{Na}$ to decrease from 30 ± 7 to 5 ± 1 mM at $V_m = -70$ mV and from 14 ± 5 to 1 ± 1 mM at $V_m = -150$ mV. $K_{0.5}^{Na}$ was also found to be voltage-dependent at any given $[\alpha MDG]_o$. Reported values for $K_{0.5}^{Na}$ measured at $V_m = -150$ mV and in the presence of 1 mM$[\alpha MDG]_o$ tend to converge toward a limiting value of 5 mM (Fig. 6; Umbach et al., 1990). $K_{0.5}^{Na}$ measured in the presence of 200 μM $[\alpha MDG]_o$ are also voltage dependent and approach toward a limiting value of 10 mM (Birnir et al., 1991). i_{max}^{Na} measured at 1 mM $[\alpha MDG]_o$ was found to be weakly voltage dependent over the complete potential range (Fig. 6*B*). Sugar uptake measurements performed with pig BBMV also showed that K_m and V_{max} for Na^+ ions was dependent upon $[D\text{-Glucose}]_o$ between 0.1 and 5 mM (Supplisson, 1988).

B. Voltage Dependence of Kinetic Parameters

In the gated-channel model applied to ion-driven (carrier-mediated) cotransport (Kessler & Semenza, 1983; Läuger & Jauch, 1986), each reaction step is described by a single energy barrier that may be influenced by the membrane potential. These reaction steps consist of (i) binding of ligands to the carrier at the external face of the membrane, (ii) translocation of ligands across the plasma membrane, (iii) release of ligands at the cytoplasmic face, and (iv) reorientation of ligand binding sites from the internal to the external face of the membrane. Two limiting cases for Na^+-driven cotransport have emerged where membrane potential may affect either Na^+ binding (high-field access channel or Na^+ well) or either carrier translocation (low-field access channel) (Läuger & Jauch, 1986). The voltage dependence of the kinetics of the Na^+/glucose cotransporter can be used therefore as a fine tool to discriminate between ion-driven transport models (Jauch & Läuger, 1986).

Voltage-clamp experiments allow one to directly extract the voltage dependence of $K_{0.5}$, i_{max} and n values as a function of membrane potential. $K_{0.5}^{\alpha MDG}$ was found to be insensitive to voltage at physiological $[Na]_o$, but as $[Na]_o$ was reduced toward 2 mM, $K_{0.5}^{\alpha MDG}$ became progressively more voltage-dependent and decreased from −10 to −150 mV (Fig. 4). In fact, the apparent sugar affinity approached the same value at high membrane potentials as that observed at saturating external Na^+ concentrations. In other words, negative membrane potential may partially compensate for the decrease in $K_{0.5}^{\alpha MDG}$ as $[Na]_o$ was reduced. Thus it appears that the apparent affinity of the cotransporter for sugar may be increased to the limiting value by either increasing $[Na]_o$ to 100 mM or increasing the membrane potential from 0 to −200 mV at low $[Na]_o$. Similar results were observed by Birnir et al. (1991). These results suggest that the voltage dependence of $K_{0.5}^{\alpha MDG}$ is due to the voltage dependence of Na^+ binding, i.e., an ion-well effect. This is supported by experiments showing a similar voltage dependence of $K_{0.5}^{Na}$ (Fig. 6), e.g., $K_{0.5}^{Na}$ decreased from ≈50 to 5 mM as the membrane potential was increased from −20 to −150 mV.

The apparent Na^+/glucose coupling coefficient n was independent of voltage, while i_{max}^{Na} and $i_{max}^{\alpha MDG}$ showed a slight voltage dependence. As with the *I-V* curves (Figs. 4 and 6), the i_{max} parameters showed voltage-sensitive and voltage-insensitive regions. In the 0- to 100-mV membrane potential range, i_{max} increased with voltage and then saturated at higher potentials. This is further evidence that there are voltage-dependent and voltage-independent steps in the transport cycle.

Studies addressing the effect of membrane potential on the kinetics of Na^+ cotransporters are important as they allow us to distinguish between two different transport models: one model involves a potential dependent translocation step (*see* Kessler & Semenza, 1983; Sanders et al., 1984), while the other involves a potential dependent Na^+ binding step, the so-called ion-well effect (Mitchell, 1969; Jauch & Läuger, 1986). In the case of the Na^+/alanine cotransporter, whole-cell current measurements have demonstrated that $K_{0.5}^{Na}$ is voltage dependent from which it was concluded that the cotrans-

porter behaved as a Na^+-well (Jauch & Läuger, 1986; Hoyer & Gögelein, 1991).

Indirect measurements of Na^+/glucose cotransporter *I-V* curves led Lapointe et al. (1986) to conclude that the potential effects were mainly at the level of the translocation step. However, Kimmich and Randles (1988) observed a "sharp" voltage dependence for K_m^{Na} when measuring sugar fluxes as a function of $[Na]_o$ and voltage, from which they inferred a Na^+-well effect. Our results show that $K_{0.5}$ and i_{max} are both voltage dependent which suggest that the potential influences both the ion binding reaction (ion-well effect) and carrier translocation.

C. Presteady-State Currents

A novel outcome of these experiments was the measurement of cotransporter presteady-state currents. These currents with a half time of ≈ 10 msec were only observed in sugar-free Na^+ medium (Fig. 10) for cRNA-injected oocytes. The addition of phlorizin or αMDG reversibly eliminated the transient currents, as did the removal of Na^+ from the bathing medium. The magnitude of these currents was influenced by the holding potential (greater for larger holding potentials). These observations suggest that transient currents are due to one of the reaction steps of the Na^+/glucose cotransporter.

Presteady-state kinetics have been reported for the Na^+/H^+ exchanger (Otsu et al., 1989) and the Na^+/glutamate cotransporter (Wierbicki, Berteloot & Roy, 1990). In both these examples, solute uptakes by membrane vesicles were measured as a function of time, and the transients were measured in the time range of seconds. In kinetic analysis of the Na^+/glucose cotransporter, presteady-state currents provide novel information to distinguish between various kinetic models (*see* companion paper).

D. Conclusion

Steady-state and presteady-state currents associated with the cloned Na^+/glucose cotransporter were measured in *Xenopus* oocytes. It is concluded from our steady-state results that both translocation and Na^+ binding and dissociation may be dependent upon membrane potential. In addition, the presteady-state currents and their modulation by Na^+, sugar and membrane potential constitute an additional tool in distinguishing transport model for the Na^+/glucose cotransporter. The companion paper presents a Na^+/glucose kinetic model based upon the electrophysiological data. Accordingly, the Na^+/glucose cotransport is described by a simultaneous mechanism with two Na^+binding sites where potential may affect both translocation and ion-binding reaction steps.

We are grateful to Dr. A. Berteloot for his thoughtful comments and to Dr. A. Pajor for carefully reading the manuscript. We thank our colleagues for discussions, and M. Bernard Tai for technical help with electronics. L. Parent was a recipient of a post-doctoral fellowship from the Medical Research Council of Canada. This work was supported by a grant from the U.S. Public Health Service DK 19567.

References

Birnir, B., Loo, D.D.F., Wright, E.M. 1991. Voltage-clamp studies of the Na^+/glucose cotransporter cloned from rabbit small intestine. *Pfluegers Arch.* **418:**79–85

Brot-Laroche, E., Supplisson, S., Delhomme, B., Alcade, A.I., Alvarado, F. 1987. Characterization of the D-glucose/Na^+ cotransport system in the intestinal brush-border membrane by using specific substrate, methyl α-D-glucopyranoside. *Biochim. Biophys. Acta* **904:**71–80

Dascal, N. 1987. The use of *Xenopus* oocytes for the study of ion channels. *CRC Crit. Rev. Biochem.* **22:**317–837

Hediger, M.A., Coady, M.J., Ikeda, T.S., Wright, E.M. 1987. Expression cloning and cDNA sequencing of the Na^+/glucose co-transporter. *Nature* **330:**379–381

Hopfer, U. 1987. Membrane transport mechanisms for hexoses and amino acids in the small intestine. *In:* Physiology of the Gastrointestinal Tract. L.R. Johnson, editor. pp. 1499–1526. Raven, New York

Hoyer, J., Gögelein, H. 1991. Sodium-alanine cotransport in renal proximal tubule cells investigated by whole-cell current recording. *J. Gen. Physiol.* **97:**1073–1094

Ikeda, T.S., Hwang, E.S., Coady, M.J., Hirayama, B.A., Hediger, M.A., Wright, E.M. 1989. Characterization of a Na^+/glucose cotransporter cloned from rabbit small intestine. *J. Membrane Biol.* **110:**87–95

Jauch, P., Läuger, P. 1986. Electrogenic properties of the sodium-alanine cotransporter in pancreatic acinar cells: II. Comparison with transport models. *J. Membrane Biol.* **94:**117–127

Jauch, P., Petersen, O.H., Läuger, P. 1986. Electrogenic properties of the sodium-alanine cotransporter in pancreatic acinar cells: I. Tight-seal whole cell recordings. *J. Membrane Biol.* **94:**99–115

Kaunitz, J.D., Wright, E.M. 1984. Kinetics of sodium D-glucose cotransport in bovine intestinal brush border vesicles. *J. Membrane Biol.* **79:**41–51

Kessler, M., Semenza, G. 1983. The small-intestinal Na^+, D-glucose cotransporter: An asymmetric gated channel (or pore) responsive to $\Delta\Psi$. *J. Membrane Biol.* **76:**27–56

Kimmich, G.A. 1990. Membrane potentials and the mechanism of intestinal Na^+-dependent sugar transport. *J. Membrane Biol.* **114:**1–27

Kimmich, G.A., Randles, J. 1984. Sodium-sugar coupling stoichiometry in chick intestinal cells. *Am. J. Physiol.* **247:**C74–C82

Kimmich, G.A., Randles, J. 1988. Na^+-coupled sugar transport: Membrane potential-dependent K_m and K_i for Na^+. *Am. J. Physiol.* **255:**C486–494

Lapointe, J.-Y., Hudson, R.L., Schultz, S.G. 1986. Current-voltage relations of sodium-coupled sugar transport across the

apical membrane of *Necturus* small intestine. *J. Membrane Biol.* **93:**205–219

Läuger, P., Jauch, P. 1986. Microscopic description of voltage effects on ion-driven cotransport systems. *J. Membrane Biol.* **91:**275–284

Misfeldt, D.S., Sanders, M.J. 1982. Transepithelial transport in cell culture: Stoichiometry of Na/phlorizin binding and Na/D-glucose cotransport. A two-step, two-sodium model of binding and translocation. *J. Membrane Biol.* **70:**191–198

Mitchell, P. 1969. Chemiosmotic coupling and energy transduction. *Theor. Exp. Biophys.* **2:**159–216

Otsu, K., Kinsella, J., Sacktor, B., Froehlich, J.P. 1989. Transient state kinetic evidence for an oligomer in the mechanism of Na^+-H^+ exchange. *Proc. Natl. Acad. Sci. USA* **86:**4818–4922.

Parent, L., Supplisson, S., Loo, D.D.F., Wright, E.M. 1990*a*. Relaxation of the Na^+/glucose cotransporter. *Biophys. J.* **57:**84 (*Abstr.*)

Parent, L., Supplisson, S., Loo, D.D.F., Wright, E.M. 1990*b*. Steady-state kinetics of the cloned Na^+/glucose cotransporter: A voltage-clamp study. *J. Am. Soc. Neph.* **1:**728 (*Abstr.*)

Parent, L., Supplisson, S., Loo, D.D.F., Wright, E.M. 1991*a*. Electrogenic properties of the cloned Na^+/glucose cotransporter. Part II: A transport model under nonrapid equilibrium conditions. *J. Membrane Biol.* **125:**63–79

Parent, L., Supplisson, S., Loo, D.D.F., Wright, E.M. 1991*b*. Electrogenic properties of the cloned Na^+/glucose cotransporter: Transport model under non rapid equilibrium. *Biophys. J.* **59:**396 (*Abstr*)

Peerce, B.E., Wright, E.M. 1984. Sodium-induced conformational changes in the glucose transporter of brush borders. *J. Biol. Chem.* **259:**14105–14112

Sanders, D., Hansen, U.-P., Gradmann, D., Slayman, C.L. 1984. Generalized kinetic analysis of ion-driven cotransport systems: A unified interpretation of selective ionic effects on Michaelis parameters. *J. Membrane Biol.* **77:**123–152

Schultz, S.G. 1986. Ion-coupled transport of organic solutes across biological membranes. *In:* Physiology of Membrane Disorders. T.E. Andreoli, J.F. Hoffman, D.D. Fanestil, and S.G. Schultz, editors. pp. 283–294. Plenum, New York

Semenza, G., Kessler, M., Hosang, M., Schmidt, U. 1984. Biochemistry of the Na^+, D-glucose cotransporter of the small intestinal brush-border membrane. *Biochim. Biophys. Acta* **779:**343–379

Smith-Maxwell, C., Bennett, E., Randles, J., Kimmich, G. 1990. Whole-cell recording of sugar-induced currents in LLC-PK_1 cells. *Am. J.Physiol.* **258:**C234-C242

Supplisson, S. 1988. Étude du caractère électrogène et de la sensibilité au voltage du transport de D-glucose couplé au sodium à travers la membrane de vésicules de bordures en brosse intestinales de cobaye et de porc. Ph.D. Thesis. Université de Paris-Sud, Centre d'Orsay

Umbach, J., Coady, M.J., Wright, E.M. 1990. Intestinal Na^+/glucose cotransporter expressed in *Xenopus* oocytes is electrogenic. *Biophys. J.* **57:**1218–1224

Weber, W.-M., Schwarz, W., Passow, H. 1989. Endogenous D-glucose transport in oocytes of *Xenopus laevis*. *J. Membrane Biol.* **111:**93–102

Wierzbicki, W., Berteloot, A., Roy, G. 1990. Presteady-state kinetics and carrier-mediated transport: A theoretical analysis. *J. Membrane Biol.* **117:**11–27

Received 12 April 1991; revised 25 June 1991